Superparamagnetic Relaxation Times for Mixed Cubic and Uniaxial Anisotropy and High Energy Barriers: II. Intermediate-to-High Damping and Uniaxial Axis in a ⟨111⟩ Direction

Andrew J. Newell
*Center for Research in Scientific Computation, Department of Marine, Earth and Atmospheric Sciences, P.O. Box 8208, North Carolina State University, Raleigh, NC 27695-8208**
(Dated: May 5, 2004)

Superparamagnetic relaxation rates are calculated for ferromagnetic particles with mixed cubic and uniaxial anisotropy. In Part I the uniaxial axis is in a ⟨001⟩ crystallographic direction, while in this article it is in a ⟨111⟩ crystallographic direction. The method is a generalization of the uniaxial theory of W. F. Brown, Jr. [Phys. Rev. **130**, 1677 (1963)] for high energy barriers and intermediate-to-high dissipation. Relaxation rates are obtained for the distribution of probability among remanent states and the resulting magnetic moment. The magnetic moment can be separated into components parallel to and perpendicular to the uniaxial easy axis with independent relaxation rates. These rates depend on the uniaxial anisotropy parameter K_u and the cubic anisotropy parameter K_1'. For oblate anisotropies ($K_u < 0$) the relaxation is nearly isotropic, but as K_u passes zero a strong anisotropy develops. If $K_1' > 0$ and $0 < K_u < 0.7611K_1'$, the effect of increasing K_u is to decrease the parallel rate and increase the perpendicular rate. The perpendicular component is identically zero for larger K_u. If $K_1' < 0$ and $0 < K_u < 0.2229|K_1'|$, there are two relaxation rates for the parallel component. One is nearly equal to the perpendicular rate and is an increasing function of K_u while the other is a decreasing function of K_u. The effect of the more rapid rate is to increase the parallel component to saturation. The parallel component then decays at the slower rate. If a sample has oriented ferromagnetic particles, it can have a superparamagnetic relaxation rate with a strong directional dependence.

PACS numbers: 76.20+q,75.20.-g

I. INTRODUCTION

In this article and part I[1] of the series (hereafter referred to as N1) I generalized the Néel-Brown theory[2,3] for superparamagnetic relaxation rates. I calculate the superparamagnetic relaxation times for ferromagnets with two anisotropy components, one cubic and one uniaxial. In N1 the easy axis is in a ⟨001⟩ crystallographic direction; in this article it is in a ⟨111⟩ direction. I assume that energy barriers are high enough to make transitions rare, and the damping is intermediate-to-high. The theory and notation is developed in N1.

II. RESULTS

Below, the same organization is used as in N1. In section II A the equilibrium solutions are calculated as functions of the ratio K_u/K_1'. In section II B the eigenvalues of the Jacobian are calculated for each solution to determine whether the solution is a minimum, maximum or saddle point. The results of section II A and II B are used in section II C to calculate the prefactor for the attempt frequency over each saddle point. In section II D the master equations are constructed and solved to give the time dependence of the probability of each state as a function of the single-barrier frequencies. Finally, the solutions for the probability are used to derive the time dependence of the magnetic moment.

A. Equilibrium States

In superparamagnetic and single-domain particles the instantaneous magnetization $\mathbf{M}$ always has magnitude $|\mathbf{M}| = M_s$, where M_s is the saturation magnetization. Equilibrium states are stationary points of the free energy with the constraint $|\mathbf{M}| = M_s$. The free energy density g depends on the direction cosines $\mathbf{M}/M_s = (\alpha, \beta, \gamma)$ of the magnetization and the anisotropy parameters K_u (uniaxial) and K_1' (cubic). With the uniaxial axis in the [111] direction,

$$g = K_u\left(1 - (\alpha+\beta+\gamma)^2/3\right) + K_1'(\alpha^2\beta^2 + \beta^2\gamma^2 + \gamma^2\alpha^2). \tag{1}$$

The case $K_1' = 0$ (pure uniaxial) was treated by Brown[3]. Assuming $K_1' \neq 0$, let $\kappa = K_u/K_1'$. The equilibrium solutions can be simplified considerably if we rotate to a coordinate system with x, y, z axes in the $[1\bar{1}0]$, $[11\bar{2}]$ and [111] directions. The new coordinates $\tilde{\mathbf{m}} = (\tilde{\alpha}, \tilde{\beta}, \tilde{\gamma})^T$ are given by $\tilde{\mathbf{m}} = R^{-1}\cdot\mathbf{m}$, where $\mathbf{m} = (\alpha, \beta, \gamma)^T$ and

$$R_{ij} = \begin{pmatrix} 1/\sqrt{2} & 1/\sqrt{6} & 1/\sqrt{3} \\ -1/\sqrt{2} & 1/\sqrt{6} & 1/\sqrt{3} \\ 0 & -2/\sqrt{6} & 1/\sqrt{3} \end{pmatrix}. \tag{2}$$

Substituting for $\mathbf{m}$ in (1), we obtain an expression for g in the tilde coordinates. This expression is even in $\tilde{\alpha}$. Substituting $\tilde{\alpha}^2 = 1 - \tilde{\beta}^2 - \tilde{\gamma}^2$ and taking derivatives with respect to $\tilde{\beta}$ and $\tilde{\gamma}$, we obtain the equilibrium equations:

$$\tilde{\gamma}\left(4\,\tilde{\beta}^2 - 1 + \tilde{\gamma}^2\right) = 0 \tag{3a}$$

$$8\,\tilde{\beta}^3 - 6\,\tilde{\beta} + 18\,\tilde{\gamma}^2\tilde{\beta} - 3\,\sqrt{2}\tilde{\gamma} + 7\,\sqrt{2}\tilde{\gamma}^3 = 6\,\sqrt{2}\,\tilde{\gamma}\kappa. \tag{3b}$$

The equations were derived using symbolic algebra (see the electronic supplement). The solutions of (3a) are $\tilde{\gamma} = 0$ and $\tilde{\gamma} = \pm(1 - 4\tilde{\beta}^2)^{1/2}$. If $\tilde{\gamma} = 0$ then $(\tilde{\alpha}, \tilde{\beta}, \tilde{\gamma}) = (\pm 1, 0, 0)$ or $(\pm 1/2, \pm\sqrt{3}/2, 0)$. These six solutions, in crystallographic coordinates, are the $\langle 1\bar{1}0\rangle$ directions that are perpendicular to the [111] direction. I will refer to them as the $1\bar{1}0_\perp$ solutions.

If the other solution of (3a), $\tilde{\gamma} = \pm(1 - 4\tilde{\beta}^2)^{1/2}$, is substituted in (3b), the result is

$$2^{1/2}\tilde{\beta}(-3+16\tilde{\beta}^2) = \mp\left(1 - 4\tilde{\beta}^2\right)^{1/2}(3\kappa - 2 + 14\tilde{\beta}^2). \tag{4}$$

Squaring both sides leads to a third order equation in $\tilde{\beta}^2$:

$$\tilde{\beta}^6 + r\tilde{\beta}^4 + s\tilde{\beta}^2 + t = 0, \tag{5}$$

where

$$r = (28\kappa - 51)/108 \tag{6}$$

$$s = (6\kappa^2 - 22\kappa + 15)/216 \tag{7}$$

$$t = -(9\kappa^2 - 12\kappa + 4)/1296. \tag{8}$$

The standard transformation[4]

$$\tilde{\beta}^2 = x - r/3 \tag{9}$$

gives the reduced form

$$x^3 + px + q = 0, \tag{10}$$

where $p = (3s - r^2)/3$ and $q = 2r^3/27 - rs/3 + t$. In terms of κ,

$$p = (188\kappa^2 - 708\kappa - 171)/34992 \tag{11}$$

$$q = -(9436\kappa^3 + 7002\kappa^2 - 621\kappa - 378)/8503056. \tag{12}$$

The discriminant of (10) is $D = (p/3)^3 + (q/2)^2$. If $D \le 0$ there are three real solutions. This is true for $-0.2229 < \kappa < 0.7611$. Outside of this range there are two complex conjugates and one real solution.

The solutions of (10) can be expressed in a variety of ways. The following expressions are chosen to ensure that the solutions (and all intermediate steps in calculating the solutions) are always real[4]. Let $R = (\mathrm{sign}(q))\sqrt{|p|/3}$. There are three cases:

$p < 0$, $D \le 0$: Let $\cos\phi = q/(2R^3)$. Then $x = -2R\cos(\phi/3 + n\pi/3)$ for $n = 0, 2, 4$.

$p < 0$, $D > 0$: Let $\cosh\phi = q/(2R^3)$. Then $x = -2R\cosh(\phi/3)$.

$p > 0$: Let $\sinh\phi = q/(2R^3)$. Then $x = -2R\sinh(\phi/3)$.

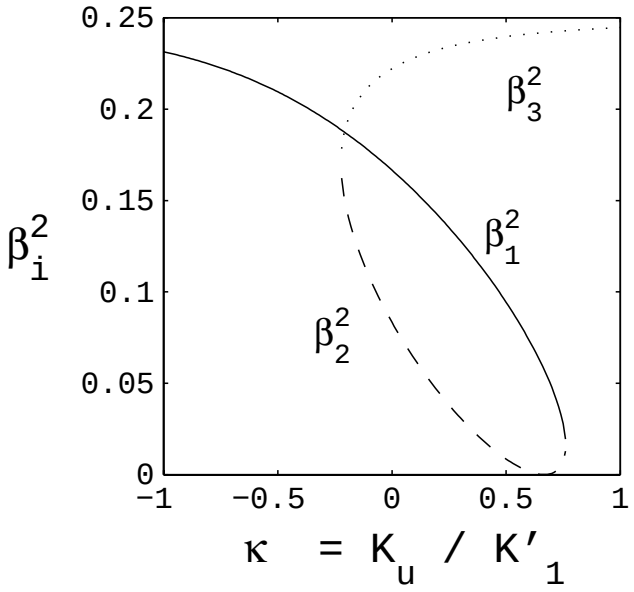

FIG. 1: Solutions of (9-12) for $\tilde{\beta}^2$. Three branches are distinguished by line type. The subscripts $1, 2, 3$ correspond to the $g100$, $g110$ and $g111$ solutions.

Unfortunately, because of the polynomial dependence of p and q on κ, the solutions are not smooth functions of κ. Jumps between curves occur when $D = 0$, or when $D < 0$ and either of p or q are zero. However, they can be rearranged (see the electronic supplement) to give three smooth solution curves. These curves are shown in Fig. 1.

Although $\tilde{\beta}^2$ is always real, $\tilde{\beta}$ could be imaginary if $\tilde{\beta}^2 < 0$. However, the solutions in Fig. 1 appear to be always positive, except perhaps for $\tilde{\beta}_2^2$. For the solution to change sign, it must cross zero, which requires that $t = 0$ in (5). The only solution for $t = 0$ is a double root $\kappa = 2/3$. Thus, $\tilde{\beta}_2^2$ touches zero but does not cross it. Below, I will choose $\tilde{\beta}_i$ to be the negative square root of $\tilde{\beta}_i^2$ for $i = 2$ and $\kappa > 2/3$ and the positive square root otherwise. This ensures that $\tilde{\beta}_2$ changes smoothly across $\kappa = 2/3$ and makes subsequent calculations simpler.

Recall that the equations for $\tilde{\beta}_i^2$ were obtained by substituting $\tilde{\alpha}^2 = 1 - \tilde{\beta}^2 - \tilde{\gamma}^2$ and $\tilde{\gamma} = \pm(1 - 4\tilde{\beta}^2)^{1/2}$. With the above conventions for $\tilde{\beta}_i$, numerical substitutions show that the value of $\tilde{\gamma}_i$ that solves (3b) is

$$\tilde{\gamma}_i = s_i\left(1 - 4\tilde{\beta}_i^2\right)^{1/2}, \tag{13}$$

where $s_i = (1, -1, -1)$. Thus, for each positive root $\tilde{\beta}_i, i = 1\ldots 3$, the equilibrium moments in the tilde coordinate system are

$$\tilde{\mathbf{m}} = \pm\left(\pm\tilde{\beta}_i\sqrt{3}, \tilde{\beta}_i, \tilde{\gamma}_i\right). \tag{14}$$

Not all the equilibrium states are obtained by the above procedure, but the remainder can be obtained by

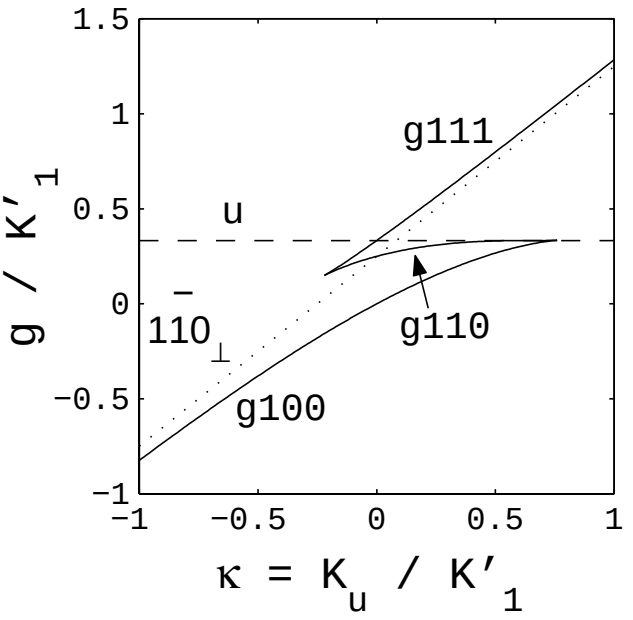

FIG. 2: Energies of the equilibrium states normalized by K_1'.

appealing to the three-fold symmetry about the [111] axis. The solutions

$$\tilde{\mathbf{m}} = \pm\left(0, -2\tilde{\beta}_i, \tilde{\gamma}_i\right). \tag{15}$$

are obtained by rotations about this axis. In crystallographic coordinates all the solutions can be written

$$\mathbf{m} = \pm\left(2\mathbf{v}^j\tilde{\beta}_i + \mathbf{u}\tilde{\gamma}_i\right), \tag{16}$$

where $\mathbf{u}$ is the unit vector in the [111] direction and $\mathbf{v}^j$ the unit vector in the $[\bar{1}\bar{1}2]$, $[2\bar{1}\bar{1}]$ or $[\bar{1}2\bar{1}]$ direction. Thus, for each solution $\tilde{\beta}_i$ there are six directions for the magnetic moment. The energies of these states are

$$g^{(i)} = \frac{K_1'}{3}\left[1 - 8\tilde{\beta}_i^2 + 28\tilde{\beta}_i^4 - 8\sqrt{2}\tilde{\beta}_i^3\tilde{\gamma}_i\right] + 4K_u\tilde{\beta}_i^2. \tag{17}$$

(See the electronic supplement). When $K_u = 0$, the solutions are $\tilde{\beta}_1 = 1/\sqrt{6}$, $\tilde{\beta}_2 = 1/(2\sqrt{3})$, and $\tilde{\beta}_3 = \sqrt{2}/3$. The corresponding magnetic moments are in the $\langle 001\rangle$, $\langle 110\rangle$, and $\langle 111\rangle$ directions (except for [111] and $[\bar{1}\bar{1}\bar{1}]$). I will refer to them as the $g100$, $g110$ and $g111$ states (the "g" stands for "generalized.").

The other equilibrium solutions for uniaxial axis in the [111] direction are the [111] and $[\bar{1}\bar{1}\bar{1}]$ directions, which I will call the u solutions. These have have energy $K_1'/3$. Finally, there are the previously mentioned $1\bar{1}0_\perp$ directions, which have energy $K_u + K_1'/4$. All of the solutions are in, or perpendicular to, one of the $(1\bar{1}0)$, $(01\bar{1})$ or $(10\bar{1})$ planes. The energies of all the states are shown in Fig. 2.

B. Stability

To determine the stability of the states, I use the same approach as in N1, rotating the coordinates so the equilibrium state is in the z direction and then obtaining the eigenvalues of the Jacobian in the perpendicular coordinates x, y. Two positive eigenvalues indicate an energy minimum, two negative eigenvalues a maximum, and mixed signs a saddle point. The matrix that maps the crystallographic coordinates onto the new coordinates is the rotation matrix $R^\perp$. For the u state, the tilde coordinates $\tilde{\alpha}, \tilde{\beta}$ are perpendicular coordinates, so $R^\perp$ is given by (2). The eigenvalues of the Jacobian are both equal to $2K_u - 4K_1'/3$. Thus, the u state is an energy minimum for $K_u > 2K_1'/3$ and a maximum for $K_u < 2K_1'/3$.

A suitable rotation matrix for the $1\bar{1}0_\perp$ states is

$$R^\perp_{ij} = \begin{pmatrix} 0 & 1/\sqrt{2} & 1/\sqrt{2} \\ 0 & 1/\sqrt{2} & -1/\sqrt{2} \\ 1 & 0 & 0 \end{pmatrix}. \tag{18}$$

The resulting eigenvalues are

$$\lambda_\pm/K_1' = -\frac{1}{2} - \kappa \pm \frac{1}{2}\left[4\kappa^2 + 4\kappa + 9\right]^{1/2}. \tag{19}$$

This has the form $a \pm \sqrt{b}$, where $b - a^2 = 2(K_1')^2 \geq 0$. Therefore, if K_1' is nonzero, there is always one positive and one negative eigenvalue, so the $1\bar{1}0_\perp$ states are always saddle points.

For each of the sets of states $g100$, $g110$ and $g111$ we need only determine the stability of one member. It is most convenient to use the state given by (15). Then $\tilde{\mathbf{m}} = \tilde{R}^\perp\mathbf{m}^\perp$, where

$$\tilde{R}^\perp_{ij} = \begin{pmatrix} 1 & 0 & 0 \\ 0 & \tilde{\gamma}_i & -2\tilde{\beta}_i \\ 0 & 2\tilde{\beta}_i & \tilde{\gamma}_i \end{pmatrix}. \tag{20}$$

The matrix that converts crystallographic to perpendicular coordinates is therefore $R^\perp = R\cdot\tilde{R}^\perp$. Applying this transformation, the eigenvalues for state i are:

$$\lambda_1^{(i)}/K_1' = \frac{4}{3}\left[-1 + 11\tilde{\beta}_i^2 - 28\tilde{\beta}_i^4 + 8\sqrt{2}\tilde{\beta}_i^3\tilde{\gamma}_i + 3\sqrt{2}\tilde{\beta}_i\tilde{\gamma}_i\right] + \kappa(2 - 8\tilde{\beta}_i^2) \tag{21a}$$

$$\lambda_2^{(i)}/K_1' = \frac{4}{3}\left[-1 + 29\tilde{\beta}_i^2 - 112\tilde{\beta}_i^4 + 32\sqrt{2}\tilde{\beta}_i^3\tilde{\gamma}_i - 3\sqrt{2}\tilde{\beta}_i\tilde{\gamma}_i\right] + \kappa(2 - 16\tilde{\beta}_i^2). \tag{21b}$$

The eigenvalues for the three states are plotted in Fig. 3. For $\kappa < -0.2229$ only the $g100$ states ($i = 1$) exist, and they are minima. As κ increases, three transitions occur. At $\kappa \approx -0.2229$ the $g110$ and $g111$ states appear; the $g110$ state is always a saddle point and the $g111$ state is a maximum or minimum as $K_1' > 0$ is positive or negative. The $g110$ state approaches the u state as κ increases, meeting it at $\kappa = 2/3$. This changes the u state from minimum to maximum ($K_1' > 0$) or the reverse ($K_1' < 0$).

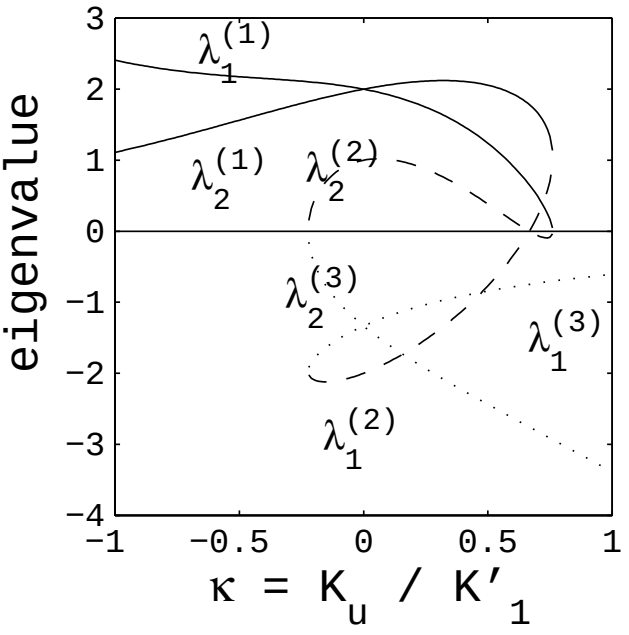

FIG. 3: The eigenvalues of the Jacobian corresponding to the three solutions in Fig. 1. The eigenvalues are normalized by K_1'.

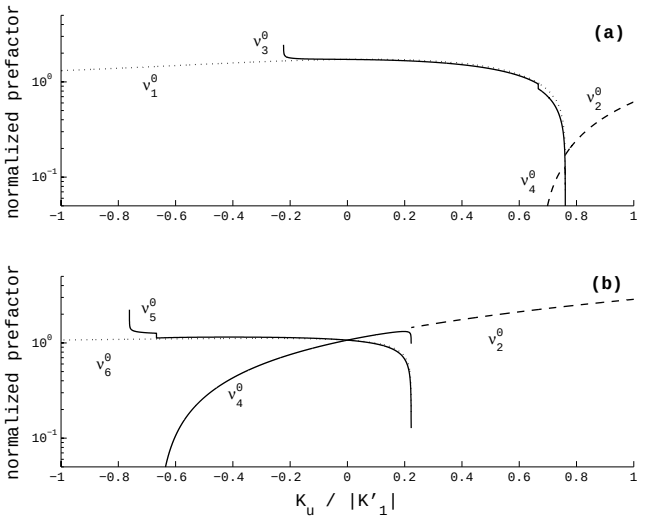

FIG. 4: Prefactors for the single-barrier relaxation rates ν_i listed in Table I. The prefactors are normalized by $2\pi M_s/|\gamma_0 K_1'|$ and the parameters $\alpha = 0.1$, $|K_1'|v/kT = 80$ are used. (a) $K_1' > 0$. (b) $K_1' < 0$.

The $g110$ state then moves towards the $g100$ state as κ continues to increase. At $\kappa = 0.7611$ the $g110$ and $g100$ states annihilate each other. This leaves the $g111$ state, which is a maximum for $K_1' > 0$ and a minimum for $K_1' < 0$.

C. Single-Barrier Relaxation Rates

The equations for the single-barrier relaxation rates ν_i were developed in N1. Given initial state i, final state j and saddle point s in between, the attempt frequency over the saddle point is

$$\nu_{ij} = \nu_{ij}^0 \exp\left[-(g_s - g_i)v/kT\right], \tag{22}$$

where v is the volume, T the temperature, and k Boltzmann's constant. The prefactor ν_{ij}^0 is given by

$$\nu_{ij}^0 = G\left(\frac{|\gamma_0'|\alpha}{2\pi M_s}\right)\left(c_1^{(i)}c_2^{(i)}\right)^{1/2}\left(\frac{c_2'}{c_1}\right)^{1/2}, \tag{23}$$

where M_s is the saturation magnetization, α the damping parameter, γ_0' the gyromagnetic factor, and

$$G = \frac{1}{2c_2'}\left\{(c_2' - c_1) + \left[(c_1 + c_2')^2 + 4\alpha^{-2}c_1c_2'\right]^{1/2}\right\}. \tag{24}$$

The parameters $c_1^{(i)}$ and $c_2^{(i)}$ are the eigenvalues of the perpendicular Jacobian for the minimum, while c_1 and $-c_2'$ are those for the saddle point (chosen so c_1 and c_2' are both positive). These eigenvalues were calculated in Section II B.

For the rest of this article a single-subscript frequency ν_i refers to a particular combination of initial state and saddle point. These variables are defined in Table I and the parameters needed to calculate them are included. The frequencies are also labelled in Figs. 6-9.

The prefactors, normalized by $2\pi M_s/|\gamma_0 K_1'|$, are displayed in Fig. 4. The normalized prefactor is dimensionless and depends on α, κ, the sign of K_1', and $|K_1'|v/kT$. For the independent variable I use $K_u/|K_1'|$ instead of κ because it is easier to interpret. Some of the prefactors diverge to zero or infinity on approaching the three values of κ (-0.2229, $2/3$ and 0.7611) at which solutions change stability. In addition, the prefactors for ν_3 ($K_1' > 0$) and ν_5 ($K_1' < 0$) have small jumps at $\kappa = 2/3$ associated with the change in connectivity of the $g110$ saddle point (compare Figures 7 and 8). As discussed in N1, these anomalies occur when the assumptions behind the Kramers theory fail. In particular, one or more second derivatives go to zero at a minimum or saddle point (Table I). Higher order expansion may not help because either the minimum or the saddle point is not in local quasiequilibrium. Thus, a numerical solution of the Fokker-Planck equation may be necessary near the critical values of κ.

The single-barrier rates are plotted in Fig. 5. Because of the strong dependence of each rate on $\exp(-(g_s - g_i)v/kT)$, the divergences in the prefactors mostly have no visible effect except very close to one of the critical values of κ. Thus, in practice they are not very important.

TABLE I: Parameters for the relaxation rate over a single barrier. Each rate is defined for a particular combination of energy minimum and saddle point. The parameters are used in (22,23,24) to determine the rate. Expressions for the $\lambda_i^{(j)}$ are given in (21).

ν	min	saddle	$c_1^{(i)}$	$c_2^{(i)}$	c_1	$-c_2'$	$(g_s - g_i)$
ν_1	$g100$	$1\bar{1}0_\perp$	$\lambda_1^{(1)}$	$\lambda_2^{(1)}$	λ_+	λ_-	$K_u + K_1'/4 - g^{(1)}$
ν_2	u	$1\bar{1}0_\perp$	$2K_u - 4K_1'/3$	$2K_u - 4K_1'/3$	λ_+	λ_-	$K_u - K_1'/12$
ν_3	$g100$	$g110$	$\lambda_1^{(1)}$	$\lambda_2^{(1)}$	$\lambda_2^{(2)\,a}$	$\lambda_1^{(2)\,a}$	$g^{(2)} - g^{(1)}$
ν_4	u	$g110$	$2K_u - 4K_1'/3$	$2K_u - 4K_1'/3$	$\lambda_1^{(2)}$	$\lambda_2^{(2)}$	$g^{(2)} - K_1'/3$
ν_5	$g111$	$g110$	$\lambda_1^{(3)}$	$\lambda_2^{(3)}$	$\lambda_1^{(2)\,a}$	$\lambda_2^{(2)\,a}$	$g^{(2)} - g^{(3)}$
ν_6	$g111$	$1\bar{1}0_\perp$	$\lambda_1^{(3)}$	$\lambda_2^{(3)}$	λ_+	λ_-	$K_u + K_1'/4 - g^{(3)}$

[a]Values for $\kappa < 2/3$. If $\kappa > 2/3$, the entries for c_1 and c_2' should be exchanged.

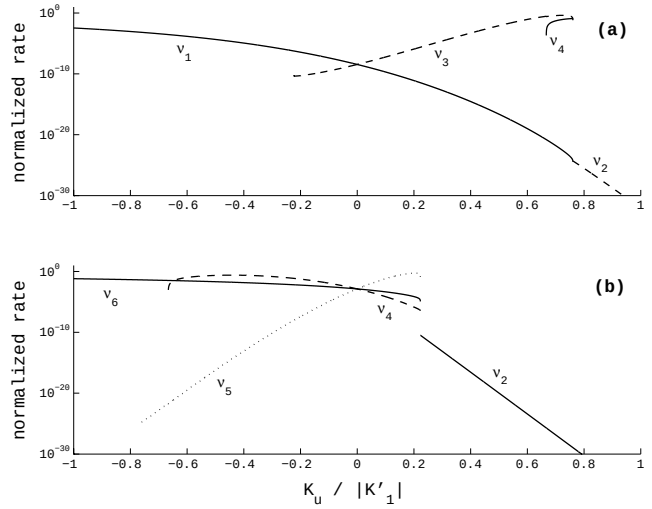

FIG. 5: Single-barrier relaxation rates ν_i for (a) Fe ($M_s = 1.72 \times 10^6\,\mathrm{kA/m}$, $K_1' = 4.8 \times 10^4\,\mathrm{Jm^{-3}}$) and (b) Ni ($M_s = 4.85 \times 10^5\,\mathrm{kA/m}$, $K_1' = -5 \times 10^3\,\mathrm{Jm^{-3}}$). In both plots, $|K_1'|v/kT = 80$, $\alpha = 0.1$ and the rates are normalized by $2\pi M_s/|\gamma_0 K_1'|$.

D. Master Equations

In this section I calculate the master equations for the probability distribution, using the methods developed in N1. Given the transition rate ν_{ij} from state i to state j for each pair of states, the master equation matrix W is constructed by taking $W_{ij} = \nu_{ji}$ for $i \neq j$ and $W_{ii} = -\sum_j \nu_{ij}$. The negative of each eigenvalue of W is a relaxation rate for the probability distribution. Following N1, I use the eigenvectors and eigenvalues of W to calculate the time evolution of the probability distribution for each state. I also explicitly calculate the time evolution of the moment. I make the calculations using symbolic algebra; the details are in the electronic supplement.

In what follows the magnetization is the average magnetization of an ensemble of identical single-domain particles. Unlike the magnetization of one of the component particles, the average can have a variable magnitude. $\mathbf{M}(t)$ can always be separated into parallel and perpendicular components: $\mathbf{M}(t)/M_s = m_\parallel(t)\mathbf{u} + \mathbf{m}_\perp(t)$, where $\mathbf{u}$ is a unit vector along the uniaxial axis. The perpendicular component $\mathbf{m}_\perp$ has a fixed direction and a simple exponential decay:

$$m_\perp(t) = m_\perp(0)\exp(-\nu_\perp t). \tag{25}$$

The parallel component has up to two relaxation rates and can be written

$$m_\parallel(t) = (m_\parallel(0) - A)\exp(-\nu_\parallel t) + A\exp(-\nu_\parallel' t). \tag{26}$$

If there is only one relaxation rate, $A = 0$ and $\nu_\parallel'$ is undefined.

1. $\kappa < -0.2229$

For $\kappa < -0.2229$ there are six $g100$ states, six $1\bar{1}0_\perp$ states, and two u states (Fig. 6). If $K_1' > 0$ the $g100$ states are minima, each connected to two neighbors by $1\bar{1}0_\perp$ saddle points. Numbering the states in counterclockwise order about the uniaxial easy axis vector $\mathbf{u}$, the transition rate matrix is

$$\nu_{ij} = \begin{bmatrix} 0 & \nu_1 & 0 & 0 & 0 & \nu_1 \\ \nu_1 & 0 & \nu_1 & 0 & 0 & 0 \\ 0 & \nu_1 & 0 & \nu_1 & 0 & 0 \\ 0 & 0 & \nu_1 & 0 & \nu_1 & 0 \\ 0 & 0 & 0 & \nu_1 & 0 & \nu_1 \\ \nu_1 & 0 & 0 & 0 & \nu_1 & 0 \end{bmatrix}, \tag{27}$$

where ν_1 is defined in Table I. The relaxation rates for the probability distribution are $4\nu_1$, $3\nu_1$ (double root), ν_1 (double root) and 0 (for the equilibrium distribution).

If an ensemble of particles are all initially in state 1, the component $m_\parallel$ has a simple exponential decay with initial component $m_\parallel = |\tilde{\gamma}_1|$ and rate $\nu_\parallel = 4\nu_1$. Thus, in (26), $A = 0$ and $\nu_\parallel'$ is undefined. The perpendicular component

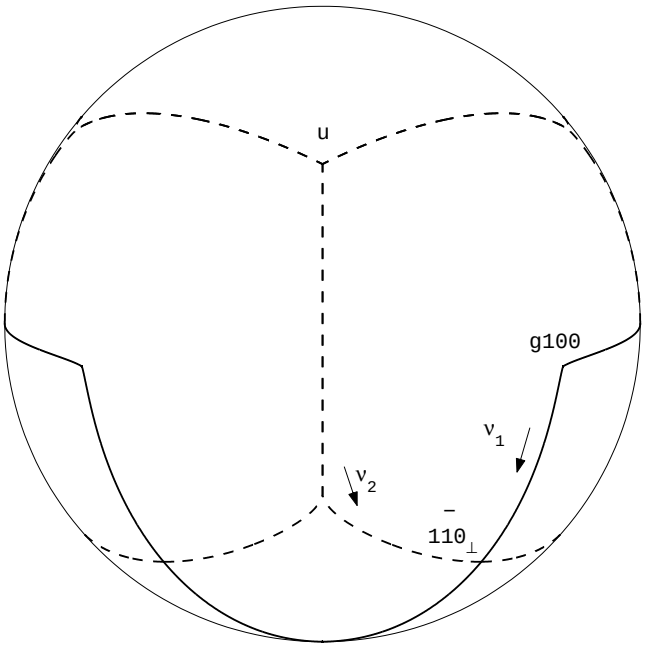

FIG. 6: Equilibrium states and their connections for $\kappa = -0.25$. The u labels a node with moment in the [111] direction. If $K_1' > 0$ the solid lines are streamlines of the energy gradient connecting saddle points with minima, while the dashed lines connect saddle points with maxima. If $K_1' < 0$ dashed and solid lines are exchanged, maxima are exchanged with minima and saddle points remain the same. Rates across the energy barriers are indicated with labels and arrows.

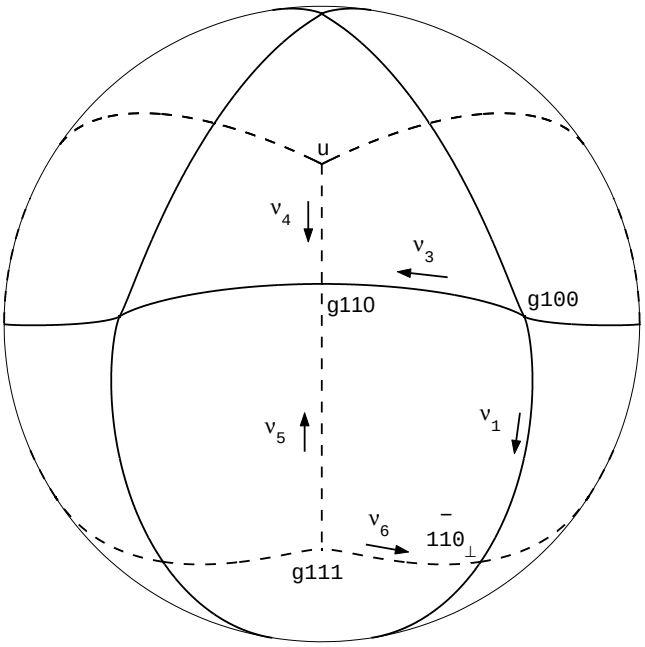

FIG. 7: Equilibrium states and their connections for $\kappa = 0.25$. The conventions are the same as for Fig. 6.

has initial value $2|\tilde{\beta}_1|$ and decays with rate $\nu_\perp = \nu_1$. The rates $4\nu_1$ and ν_1 are only two of the three relaxation rates for the probability distribution. The third, $3\nu_3$, has no effect on the moment because its relaxation mode affects both ends of each axis equally.

If $K_1' < 0$ the minima are the two u states, connected by six $1\bar{1}0_\perp$ saddle points. If all particles are initially in state 1, $m_\parallel = 1$ and the relaxation rate is $\nu_\parallel = 12\nu_2$. The rate $\nu_\perp$ is undefined because the perpendicular component is identically zero.

2. $-0.2229 < \kappa < 2/3$

As κ crosses -0.2229 the $g111$ and $g110$ states form and move apart. In Fig. 7, for $\kappa = 0.25$, they are well away from each other. For $K_1' > 0$ each $g100$ minimum is connected by $g110$ saddle points to two $g100$ states in the same hemisphere (that is, same u component). It is also connected by $1\bar{1}0_\perp$ saddle points to two $g100$ states in the other hemisphere. If the $g110$ states are numbered in a counterclockwise order about the **u** direction,

$$\nu_{ij} = \begin{bmatrix} 0 & \nu_1 & \nu_3 & 0 & \nu_3 & \nu_1 \\ \nu_1 & 0 & \nu_1 & \nu_3 & 0 & \nu_3 \\ \nu_3 & \nu_1 & 0 & \nu_1 & \nu_3 & 0 \\ 0 & \nu_3 & \nu_1 & 0 & \nu_1 & \nu_3 \\ \nu_3 & 0 & \nu_3 & \nu_1 & 0 & \nu_1 \\ \nu_1 & \nu_3 & 0 & \nu_3 & \nu_1 & 0 \end{bmatrix}, \tag{28}$$

If all particles are initially in state 1 then $m_\parallel(0) = |\tilde{\gamma}_1|$, $\nu_\parallel = 4\nu_1$, $\mathbf{m}_\perp(0) = 2|\tilde{\beta}_1|$ and $\nu_\perp = \nu_1 + 3\nu_3$. Another rate, $3(\nu_1 + \nu_3)$, has no effect on the moment.

If $K_1' < 0$ there are two u minima and six $g111$ minima. Each u minimum is connected to three $g111$ minima by $g110$ saddle points while each $g111$ minimum is connected to two others by $1\bar{1}0_\perp$ saddle points. If the states are numbered 1 for one u state, $2-7$ for the $g111$ states and 8 for the other u state, with state 2 being connected to state 1,

$$\nu_{ij} = \begin{bmatrix} 0 & \nu_4 & 0 & \nu_4 & 0 & \nu_4 & 0 & 0 \\ \nu_5 & 0 & \nu_6 & 0 & 0 & 0 & \nu_6 & 0 \\ 0 & \nu_6 & 0 & \nu_6 & 0 & 0 & 0 & \nu_5 \\ \nu_5 & 0 & \nu_6 & 0 & \nu_6 & 0 & 0 & 0 \\ 0 & 0 & 0 & \nu_6 & 0 & \nu_6 & 0 & \nu_5 \\ \nu_5 & 0 & 0 & 0 & \nu_6 & 0 & \nu_6 & 0 \\ 0 & \nu_6 & 0 & 0 & 0 & \nu_6 & 0 & \nu_5 \\ 0 & 0 & \nu_4 & 0 & \nu_4 & 0 & \nu_4 & 0 \end{bmatrix}, \tag{29}$$

The nonzero relaxation rates are $\nu_5+3\nu_4$, $\nu_5+3\nu_6$ (double root), $\nu_5+\nu_6$ (double root), and $\nu_\pm$, where

$$\nu_\pm = (\beta \pm \sqrt{\alpha})/2, \tag{30}$$

and

$$\alpha = (3\nu_4 - 4\nu_6)^2 + \nu_5^2 + 6\nu_5\nu_4 + 8\nu_5\nu_6 \tag{31a}$$
$$\beta = \nu_5 + 3\nu_4 + 4\nu_6. \tag{31b}$$

Of the relaxation rates, only $\nu_\pm$ affect $m_\parallel$, the component of the moment parallel to the uniaxial axis; and only $\nu_5+\nu_6$ affects the perpendicular component $\mathbf{m}_\perp$. The rates $\nu_\pm$ do not affect $\mathbf{m}_\perp$ because their relaxation modes (as indicated by the eigenvectors) include probability flow from the u state equally distributed among the nearest three $g111$ states. The u state and the $g111$ states have a net perpendicular component of zero, so $\mathbf{m}_\perp$ is not affected. Similarly, $\nu_5+\nu_6$ does not affect $m_\parallel$ because, despite the contribution of ν_5, the relaxation mode does not transfer any probability to the u state.

There are two kinds of state, u and $g111$, and $\mathbf{m}(t)$ depends on the initial state. For example, suppose all particles are in state 1 (a u state). From this state there is a probability flow with rate ν_4 into the nearest three $g111$ states (Fig. 7). These states are numbered 2, 4 and 6. The initial rate of change in probability is therefore $\dot{\mathbf{n}}(0) = (-3\nu_4, \nu_4, 0, \nu_4, 0, \nu_4, 0, 0)$ (the dot indicates a time derivative). Since the parallel components of the u state and $g111$ states are 1 and $|\tilde{\gamma}_3|$, $\dot{m}_\parallel(0) = 3\nu_4(|\tilde{\gamma}_3|-1)$. This is always zero or negative because $|\tilde{\gamma}_3| \le 1$, so $m_\parallel$ always decreases initially. This is to be expected because all other remanent states have a lower component in the $\mathbf{u}$ direction. The other component, $\mathbf{m}_\perp$, remains zero because of the symmetry.

The derivation of the time dependence of $m_\parallel$ is very messy, and is left to the electronic supplement. The result is that $m_\parallel(0) = 1$, $\nu_\parallel = \nu_-$, $\nu'_\parallel = \nu_+$, and

$$A = \frac{3\nu_4 - \nu_-}{\sqrt{\alpha}} - \frac{3\nu_4}{\sqrt{\alpha}}|\tilde{\gamma}_3|. \tag{32}$$

The first term in A is the contribution of relaxation between u states while the second term is that of relaxation between $g111$ states.

If all particles are in state 2 (a $g111$ state), $\dot{\mathbf{n}}(0) = (\nu_5, -\nu_5 - 2\nu_6, \nu_6, 0, 0, 0, \nu_6, 0)$. Thus, $\dot{m}_\parallel(0) = \nu_5 - |\tilde{\gamma}_3|(\nu_5 + 4\nu_6)$. Now $m_\parallel$ can increase or decrease initially, depending on the value of $|\tilde{\gamma}_3|$. As for the perpendicular component, state 2 has component $2|\tilde{\beta}_3|$, state 1 has component zero, and states 3 and 7 have components $|\tilde{\beta}_3|$. Thus, $\dot{\mathbf{m}}_\perp = -2|\tilde{\beta}_3|(\nu_5+\nu_6)$.

Solving for the time dependence of the moment, the perpendicular component has initial value $m_\perp(0) = 2|\tilde{\beta}_3|$ and relaxation rate $\nu_\perp = \nu_5 + \nu_6$, while for the parallel component $m_\parallel(0) = |\tilde{\gamma}_3|$, $\nu_\parallel = \nu_-$, $\nu'_\parallel = \nu_+$, and

$$A = -\frac{\nu_5}{\sqrt{\alpha}} + \frac{\nu_+ - 3\nu_4}{\sqrt{\alpha}}|\tilde{\gamma}_3|. \tag{32$'$}$$

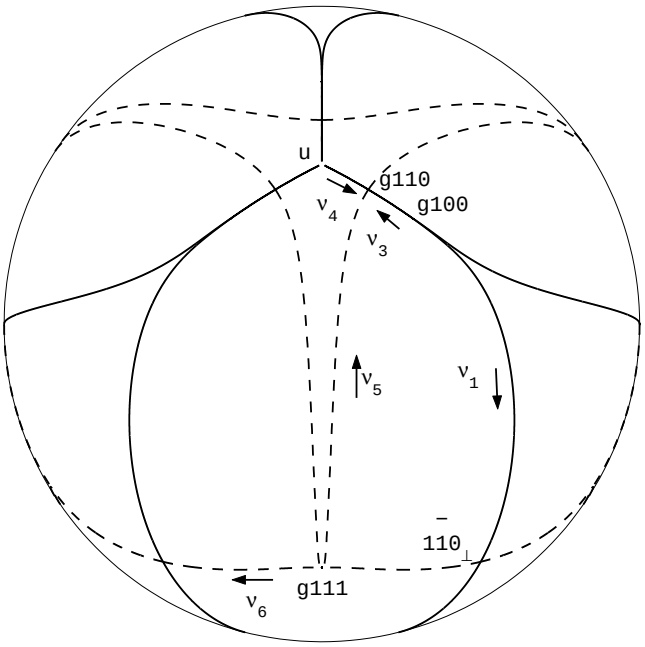

FIG. 8: Equilibrium states and their connections for $\kappa = 0.75$. The conventions are the same as for Fig. 6.

Again, the first term in A comes from relaxation between u states and the second from relaxation between $g111$ states.

3. $2/3 < \kappa < 0.7611$

As κ crosses 2/3 the $g110$ states touch the u direction and then move away again, while the u state changes stability (Fig. 8). If $K'_1 > 0$ the u state is now a minimum and is connected to the nearest $g100$ states, while those states are only directly connected to $g100$ states in the other hemisphere. Number the states 1 for the u state, $2-7$ for the $g100$ states (with 2 being connected to the u state), and 8 for the other u state. The geometry is then the same as for $-0.2229 < \kappa < 2/3$ and $K'_1 < 0$, with $g111$ states replaced by $g100$ states. Thus, ν_5 replaced by ν_3, ν_6 by ν_1 and $\tilde{\gamma}_3$ by $\tilde{\gamma}_1$. The frequencies $\nu_\pm$ are given by (30) with (31) replaced by

$$\alpha = (3\nu_4 - 4\nu_1)^2 + \nu_3^2 + 6\nu_3\nu_4 + 8\nu_3\nu_1 \tag{31a'}$$
$$\beta = \nu_3 + 3\nu_4 + 4\nu_1. \tag{31b'}$$

If all the moments are initially in the u direction, $m_\parallel(0) = 1$, $\nu_\parallel = \nu_-$, $\nu'_\parallel = \nu_+$, and

$$A = \frac{3\nu_4 - \nu_-}{\sqrt{\alpha}} - \frac{3\nu_4}{\sqrt{\alpha}}|\tilde{\gamma}_1|. \tag{32$''$}$$

The perpendicular component is identically zero.

If the initial state is $g100$, $m_\parallel(0) = |\tilde{\gamma}_1|$, $\nu_\parallel = \nu_-$,

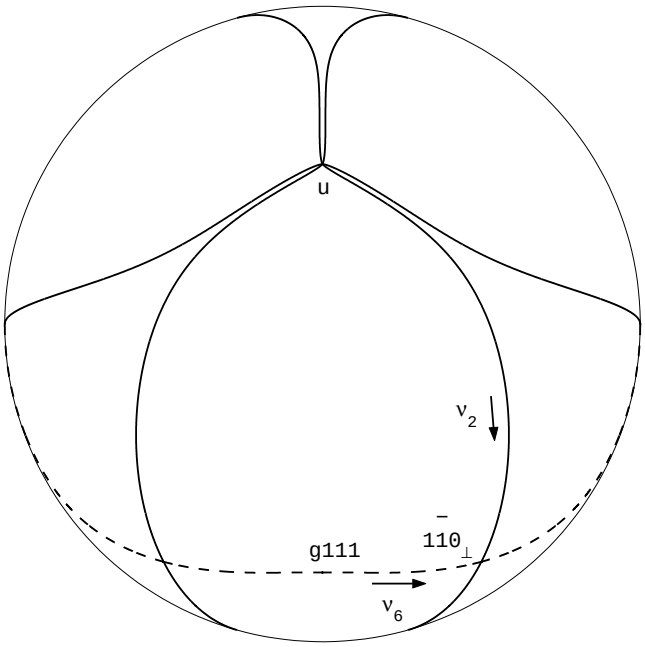

FIG. 9: Equilibrium states and their connections for $\kappa = 1$ and easy axis in the [111] direction. The conventions are the same as for Fig. 6.

$\nu'_\parallel = \nu_+$, and

$$A = -\frac{\nu_3}{\sqrt{\alpha}} + \frac{\nu_+ - 3\nu_4}{\sqrt{\alpha}}|\tilde{\gamma}_1|, \qquad (32''')$$

The coefficients for the perpendicular component are $m_\perp(0) = 2|\tilde{\beta}_1|$ and $\nu_\perp = \nu_1 + \nu_3$.

If $K'_1 < 0$ there are six $g111$ minima, each connected to two nearest neighbors by $1\bar{1}0_\perp$ saddle points, and to two next-nearest-neighbors by $g110$ saddle points. Thus,

$$\nu_{ij} = \begin{bmatrix} 0 & \nu_6 & \nu_5 & 0 & \nu_5 & \nu_6 \\ \nu_6 & 0 & \nu_6 & \nu_5 & 0 & \nu_5 \\ \nu_5 & \nu_6 & 0 & \nu_6 & \nu_5 & 0 \\ 0 & \nu_5 & \nu_6 & 0 & \nu_6 & \nu_5 \\ \nu_5 & 0 & \nu_5 & \nu_6 & 0 & \nu_6 \\ \nu_6 & \nu_5 & 0 & \nu_5 & \nu_6 & 0 \end{bmatrix}. \qquad (34)$$

There are three relaxation rates for the probability distribution: $4\nu_6$, $\nu_6 + 3\nu_5$ and $3(\nu_5 + \nu_6)$. For the moment, $m_\parallel(0) = |\tilde{\gamma}_3|$, $\nu_\parallel = 4\nu_6$, $m_\perp(0) = 2|\tilde{\beta}_3|$ and $\nu_\perp = \nu_6 + 3\nu_5$.

4. $\kappa > 0.7611$

As κ crosses 0.7611 the $g110$ and $g100$ states meet and annihilate each other. This leaves the u, $g111$ and $1\bar{1}0_\perp$ states. If $K'_1 > 0$ the minima are the two u states, connected to each other by six $1\bar{1}0_\perp$ saddle points (Fig. 9). Thus, $m_\parallel(0) = 1$, $\nu_\parallel = 12\nu_2$ and the perpendicular component is zero.

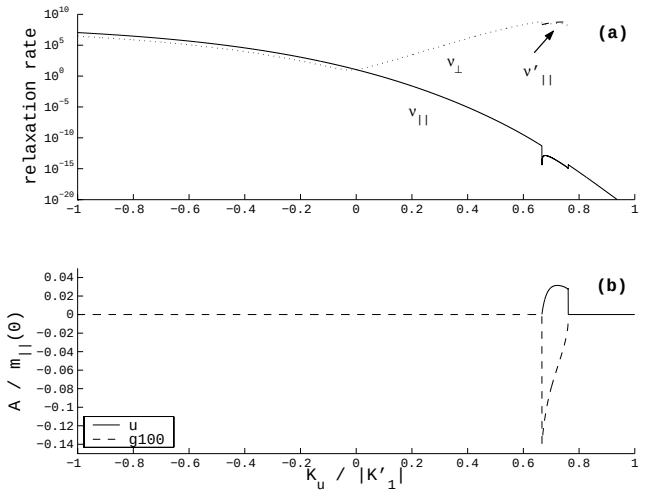

FIG. 10: (a) Relaxation rates for iron (same parameters as in Fig. 5a). (b) Parameter A in the prefactor for rates $\nu_\parallel$, $\nu'_\parallel$. As depicted, some rates are only defined for a particular starting state.

If $K'_1 < 0$ there are six $g111$ minima, each connected to two nearest neighbors across $1\bar{1}0_\perp$ saddle points. The geometry is the same as for $\kappa < -0.2229$ and $K'_1 > 0$, so $m_\parallel(0) = |\tilde{\gamma}_3|$, $\nu_\parallel = 4\nu_6$, $m_\perp(0) = 2|\tilde{\beta}_3|$ and $\nu_\perp = \nu_6$.

III. DISCUSSION

The time evolution of the magnetization is given by (25) for the perpendicular component and (26) for the parallel component. The parameters for these equations, including the initial values of the moment, relaxation rates, and prefactor A, are summarized in Table II. I have also provided a MATLAB® function in the electronic supplement to calculate them.

The relaxation rates and prefactor A are plotted in Fig. 10 for iron (an example of $K'_1 > 0$). When $K_u < 0$ the changes in moment are dominated by flow between $g100$ states across $1\bar{1}0_\perp$ barriers (rate ν_1). This determines both the parallel and perpendicular components, so $\nu_\parallel = \nu_\perp$. Once K_u is positive, flow across $g110$ barriers (rate ν_3) becomes faster. This dominates the perpendicular component, but does not affect the parallel component, so the latter is still determined by the slower rate ν_1. As K_u increases $\nu_\parallel$ decreases and $\nu_\perp$ increases.

For K_u between 2/3 and 0.7611 there are two kinds of states, u and $g100$. There are now two relaxation rates for $m_\parallel$, but still only one for $\mathbf{m}_\perp$ (as discussed in section II D 2 for $K'_1 < 0$). An example of the time dependence of $m_\parallel$ for this case is shown in Fig. 11. The relaxation occurs in two stages. First, a local equilibrium is established between the u state and the three $g100$ states in the same hemisphere. By local equilibrium I mean that

TABLE II: Parameters that determine the time dependence of the magnetization in (25-26).

sign(K_1')	$K_u/\lvert K_1'\rvert$	Initial state	$m_\parallel(0)$	$A\sqrt{\alpha}$	$\nu_\parallel$	$\nu_\parallel'$	$m_\perp(0)$	$\nu_\perp$
1	$(-\infty,-0.2229)$	$g100$	$\lvert\tilde{\gamma}_1\rvert$	0	$4\nu_1$	—	$2\lvert\tilde{\beta}_1\rvert$	ν_1
1	$(-0.2229,2/3)$	$g100$	$\lvert\tilde{\gamma}_1\rvert$	0	$4\nu_1$	—	$2\lvert\tilde{\beta}_1\rvert$	$\nu_1+3\nu_3$
1	$(2/3,0.7611)$	$g100$	$\lvert\tilde{\gamma}_1\rvert$	$-\nu_3+(\nu_+-3\nu_4)\lvert\tilde{\gamma}_1\rvert^a$	${\nu_-}^a$	${\nu_+}^a$	$2\lvert\tilde{\beta}_1\rvert$	$\nu_1+\nu_3$
1	$(2/3,0.7611)$	u	1	$3\nu_4-\nu_--3\nu_4\lvert\tilde{\gamma}_1\rvert^a$	${\nu_-}^a$	${\nu_+}^a$	0	—
1	$(0.7611,\infty)$	u	1	0	$12\nu_2$	—	0	—
-1	$(-\infty,-0.7611)$	$g111$	$\lvert\tilde{\gamma}_3\rvert$	0	$4\nu_6$	—	$2\lvert\tilde{\beta}_3\rvert$	ν_6
-1	$(-0.7611,-2/3)$	$g111$	$\lvert\tilde{\gamma}_3\rvert$	0	$4\nu_6$	—	$2\lvert\tilde{\beta}_3\rvert$	$3\nu_5+\nu_6$
-1	$(-2/3,0.2229)$	$g111$	$\lvert\tilde{\gamma}_3\rvert$	$-\nu_5+(\nu_+-3\nu_4)\lvert\tilde{\gamma}_3\rvert^b$	${\nu_-}^b$	${\nu_+}^b$	$2\lvert\tilde{\beta}_3\rvert$	$\nu_5+\nu_6$
-1	$(-2/3,0.2229)$	u	1	$3\nu_4-\nu_--3\nu_4\lvert\tilde{\gamma}_3\rvert^b$	${\nu_-}^b$	${\nu_+}^b$	0	—
-1	$(0.2229,\infty)$	u	1	0	$12\nu_2$	—	0	—

[a] where $\nu_\pm$ are given by (30) and α,β by (31′)
[b] where $\nu_\pm$ are given by (30) and α,β by (31)

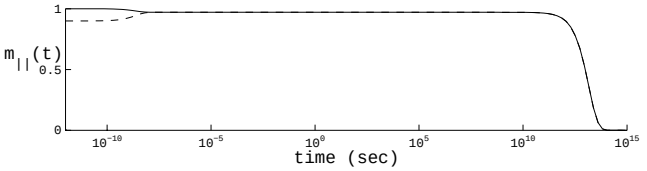

FIG. 11: Time evolution of the parallel component of the moment. Solid line: initial state is u. Dashed line: initial state is $g100$.

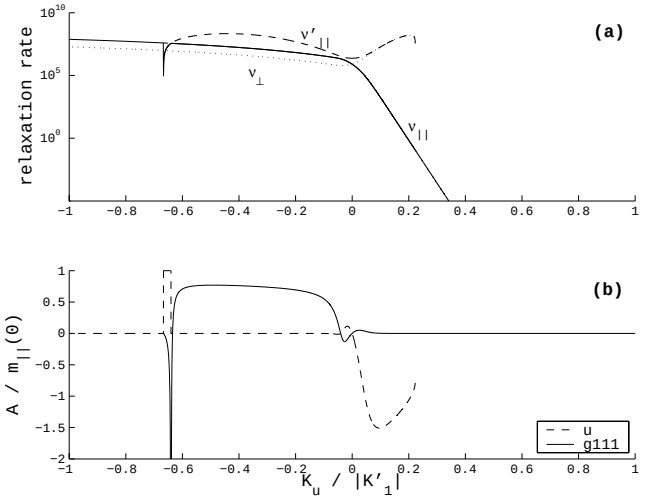

FIG. 12: (a) Relaxation rates for nickel (same parameters as in Fig. 5b). (b) Parameter A in the prefactor for rates $\nu_\parallel$, $\nu_\parallel'$. As depicted, some rates are only defined for a particular starting state.

the detailed balance condition[5] is satisfied between these four states. This leads to a decrease in $m_\parallel$ when the initial state is the u state and an increase when the initial state is $g100$ (the latter being reflected in the small negative value of A). This process occurs over a time scale $\left(\nu_\parallel'\right)^{-1}$. Since the quasi-equilibrium distribution is the same for both initial states, the moment is subsequently independent of the initial state. There is then a flow from one hemisphere to the other over the much longer time scale of $\left(\nu_\parallel\right)^{-1}$.

For $K_u > 0.7611K_1'$ the only remanent states are u states. There is then no perpendicular component and the parallel component is governed by a straightforward uniaxial-type relaxation with rate $12\nu_2$.

The relaxation rates and prefactor A are plotted in Fig. 12 for nickel ($K_1' < 0$). The $g111$ state is the only stable state for $K_u < -2/3|K_1'|$, the u state is the only stable state for $K_u > 0.2229|K_1'|$, and in between the states coexist. Thus, the overlap is much greater than for $K_1' > 0$. The rate $\nu_\parallel$ is always defined but $\nu_\perp$ is only defined where the $g111$ state is stable. In the overlap region there are two relaxation rates for $m_\parallel$. As for $K_1' > 0$, rates $\nu_\parallel$ and $\nu_\perp$ are nearly equal when $K_u < 0$ and diverge when $K_u > 0$. Where they diverge, $\nu_\parallel' \approx \nu_\perp$.

When $K_u < 0$, ν_5 (the rate for crossing $g110$ barriers from $g111$ states) is much smaller than the other two single-barrier rates, ν_4 and ν_6. This, with the equations for $\nu_\parallel$ and $\nu_\parallel'$, implies that $\nu_\parallel' \approx \max(3\nu_4, 4\nu_6)$ and $\nu_\parallel \approx \min(3\nu_4, 4\nu_6)$. Over a very narrow interval between $K_u = -2/3|K_1'|$ and the point where $3\nu_4 = 4\nu_6$, the curves appear to cross. In reality, they bend sharply away from each other. To see this, one would need to magnify the plot by orders of magnitude.

The single-state regions are straightforward, so I will focus on the overlap region. For $-2/3|K_1'| < K_u < 0.2229|K_1'|$, the shape of the curve $m_\parallel(t)$ depends on whether the initial state is u or $g111$. The relationship between the curves depends on the energies of the states and the relaxation rates $\nu_\parallel$ and $\nu_\parallel'$. Three examples are shown in Fig. 13.

For $K_u < 0$, the $g111$ states have lower energy than the u states, so the probability flows towards the $g111$ states. Thus, the moment decreases more quickly if the initial state is u. For $K_u = -0.64|K_1'|$, there are sharp swings in A, but this has little effect because $\nu_\parallel \approx \nu_\parallel'$.

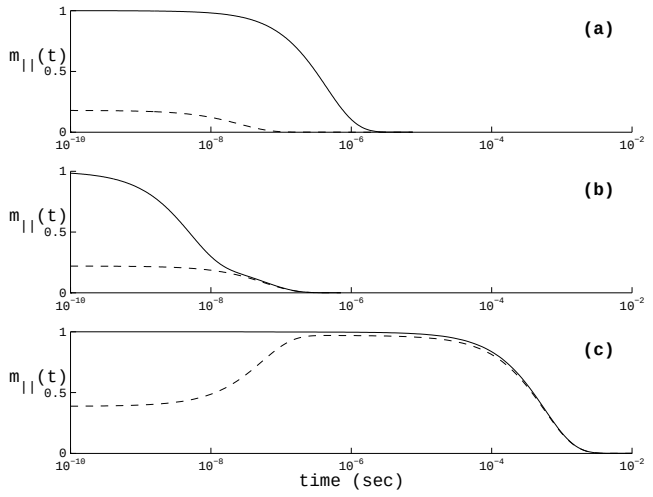

FIG. 13: Time evolution of the parallel component of the moment for $K_1' < 0$ and (a) $K_u = -0.64|K_1'|$ (b) $K_u = -0.4|K_1'|$ (c) $K_u = 0.1|K_1'|$. Solid line: initial state is u. Dashed line: initial state is $g111$.

In Fig. 13a, both curves have a similar single-exponent decay.

In Fig. 13b, $\nu_\parallel$ and $\nu_\parallel'$ are not equal, and there is a partial separation of the rates. On the time scale $(\nu_\parallel')^{-1}$ the probability flows from the u state to the nearest three $g111$ states. The separation between rates is not enough for local equilibrium to be established, but the $g111$ states are nearly saturated, so the curves for u and $g111$ initial states converge. Subsequently the moment decays with the rate $\nu_\parallel$.

For $K_u > 0$ the u state has the lowest energy. First, on the time scale $(\nu_\parallel')^{-1}$, the $g111$ states decay to the u states. In Fig. 13c the separation between rates is enough for local equilibrium to be established. The magnetization becomes saturated in the **u** direction and then decays with rate $\nu_\parallel$.

In this article the uniaxial axis is always in a $\langle 111\rangle$ crystallographic directions; in N1 it is in a $\langle 001\rangle$ direction. How do the relaxation rates compare? For $K_u < 0$, the parallel rates for the two geometries are similar, increasing slowly as K_u decreases. However, in the $\langle 001\rangle$ geometry the parallel component only exists down to a critical negative value of $K_u/|K_1'|$. The perpendicular rates are very different. They remain close to the parallel rate in the $\langle 111\rangle$ geometry but drop by orders of magnitude as K_u decreases in the $\langle 001\rangle$ geometry.

For $K_u > 0$ the relaxation rates are less dependent on the orientation of the easy axis. In all cases, as K_u increases one parallel rate $\nu_\parallel$ decreases (if more rapidly for the $\langle 111\rangle$ geometry) and the perpendicular rate increases. All perpendicular components have a critical value of $K_u/|K_1'|$ at which they disappear. This critical value is larger for the $\langle 001\rangle$ easy axis orientation.

Another difference between the geometries is the second relaxation rate for $m_\parallel$ when the uniaxial axis is in a $\langle 111\rangle$ direction. Either $\nu_\parallel$ or $\nu_\parallel'$ are very close to $\nu_\perp$, so there are effectively just two relaxation rates for the moment. However, the effects of the relaxation modes associated with $\nu_\parallel$ and $\nu_\parallel'$ can be very different. When $K_1' < 0$ and $K_u > 0$, the moment increases to saturation at the rate $\nu_\parallel'$ before decreasing at the rate $\nu_\parallel$.

The initial values and relaxation rates listed in Table II have been derived for samples in which all the particles are oriented the same way and start out in the same state. If there is more than one initial state, the magnetic moment is the sum of the moment vectors for each state. If the orientations vary, the moment must be integrated over the distribution of orientations. This is fairly straightforward if there is only one type of remanent state (for example, $g111$) because then all particles still have the same relaxation rates $\nu_\parallel$ and $\nu_\perp$. Only the initial value of the moment changes. It is more complicated if there are two types of remanent state because they have different time dependence, at least until a local equilibrium is established. The initial distribution between the two kinds of state can also be difficult to calculate for a given magnetic experiment.

The theory developed in this article and in N1 has the most striking consequences for samples with oriented particles. If $K_u > 0$ and all the uniaxial easy axes are aligned, there can be a strong anisotropy in the relaxation rate, with relaxation being much faster if the particles are magnetized perpendicular to the easy axes than if they are magnetized parallel. Indeed, in the latter case the magnetization can even increase to saturation before decreasing. These changes also imply a rotation of the moment towards the easy axis.

IV. CONCLUSIONS

In two articles I have calculated superparamagnetic relaxation times for combined cubic and uniaxial anisotropy. In part I the uniaxial axis is in a $\langle 001\rangle$ direction while in this part it is in a $\langle 111\rangle$ direction. The new theory departs from the Néel-Brown theory[2,3] in some striking ways. Instead of one relaxation rate for the distribution of probability between states, there are up to five. However, some relaxation modes do not affect the magnetic moment. Those that do are anisotropic, so that components parallel to the uniaxial easy axis and perpendicular to it have different relaxation rates. When the uniaxial anisotropy is prolate ($K_u > 0$) the parallel rate decreases as K_u increases while the perpendicular rate increases. At a critical value of $K_u/|K_1'|$, the perpendicular component disappears.

The $\langle 111\rangle$ orientation also differs from the $\langle 001\rangle$ orientation in significant respects. When the uniaxial anisotropy is oblate ($K_u < 0$), the rates for parallel and perpendicular components remain close together instead of diverging. Also, the parallel component can have two relaxation rates. When $K_1' > 0$ and $0 < K_u < 0.2229|K_1'|$

the faster relaxation mode saturates the parallel component instead of decreasing it.

The multiple relaxation modes have some important implications. A single particle can have more than one superparamagnetic/single-domain critical size and more than one blocking temperature. Between critical sizes, a local equilibrium is established between some of the remanent states. This reduces the remanence. Finally, if a sample has oriented particles, the relaxation rate depends on direction, and at the faster rate the magnetic moment will rotate. The latter predictions can also be expected to apply to particles above the single-domain size range.

Acknowledgments

This research was supported by Grants EAR-0208446 (Earth Sciences Division of the National Science Foundation) and NAG5-13465 (NASA Exobiology Program).

---

* Andrew_Newell@ncsu.edu; http://www4.ncsu.edu/~ajnewell/index.html

[1] A. J. Newell (2004), submitted to Physical Review B.

[2] L. Néel, Ann. Géophys. **5**, 99 (1949), translated in Nicholas Kurti, editor, *Selected Works of Louis Néel*, Gordon and Breach, New York, 1988, pages 407–427.

[3] W. F. Brown, Jr., Phys. Rev. **130**, 1677 (1963).

[4] I. Bronshtein and K. Semendyayev, *Handbook of Mathematics* (Van Nostrand Reinhold, New York, 1985), English translation edited by K. A. Hirsch.

[5] N. G. van Kampen, *Stochastic Processes in Physics and Chemistry* (North-Holland, New York, 1981), 419 pp.

*